Active Faulting in the Gulf of Aqaba: New Knowledge from the Mw 7.3 Earthquake of 22 November 1995

Yann Klinger, Luis Rivera, Henri Haessler, Jean-Christophe Maurin

Bulletin of the Seismological Society of America, 89, 4, pp. 1025–1036, August 1999

Active Faulting in the Gulf of Aqaba: New Knowledge from the M_W 7.3 Earthquake of 22 November 1995

by Yann Klinger, Luis Rivera, Henri Haessler, and Jean-Christophe Maurin

Abstract On 22 November 1995 the largest earthquake instrumentally recorded in the area, with magnitude M_W 7.3, occurred in the Gulf of Aqaba. The main rupture corresponding to the strike-slip mechanism is located within the gulf of Aqaba, which forms the marine extension of the Levantine fault, also known as the Dead Sea fault. The Levantine fault accommodates the strike-slip movement between the African plate and the Arabian plate. The Gulf of Aqaba itself is usually described as the succession of three deep pull-apart basins, elongated in the N–S direction. Concerning historical seismicity, only two large events have been reported for the last 2000 years, but they are still poorly constrained. The seismicity recorded since installation of regional networks in the early 1980s had been characterized by a low background level punctuated by brief swarmlike activity a few months in duration. Three swarms have already been documented in the Gulf of Aqaba in 1983, 1990, and 1993, with magnitudes reaching at most 6.1 (M_W). We suggest that the geometry of the rupture for the 1995 event is related to the spatial distribution of these previous swarms. Body-wave modeling of broadband seismograms from the global network, along with the analysis of the aftershock distribution, allow us to propose a well-constrained model for the rupture process. Northward propagation of the rupture has been found. We have demonstrated that three successive subevents are necessary to obtain a good fit between observed and synthetic wave forms. The total seismic moment released was 7.42×10^{19} N-m. The location of the subevents shows that the three stages of the rupture involve three different segments within the gulf. Substantial surface breakage showing only normal motion (up to 20 cm) affecting beachrock was observed along the Egyptian coast. We show that these ruptures are only a secondary feature and are in no case primary ruptures. The stress tensor derived from striations collected in quaternary sediments shows radial extension. This result supports landsliding of the beach terraces under the action of the earthquake shaking.

Introduction

A strong earthquake, M_W 7.3, occurred in the Gulf of Aqaba on 22 November 1995. The epicenter of the earthquake was off-shore, about 60 km from the head of the gulf where the cities of Aqaba (Jordan) and Eilat (Israel) lie. In these cities a few buildings were damaged, and a small wave swept the beach according to witnesses. More extensive destruction was reported in the city of Nuweyba (Sinai, Egypt) on the central part of the western coast, where several modern houses, built with reinforced concrete, were completely destroyed. This earthquake is the largest event ever recorded in the Gulf of Aqaba since the beginning of instrumentally recorded seismicity.

The Gulf of Aqaba belongs to the Levantine fault system (also called the Dead Sea fault) and is located at its southern extremity. The Levantine fault is considered to be a plate boundary of the transform type between the African plate and the Arabian shield, which slides along this limit in its northward motion. More than 1000 km in length, the Levantine fault connects the spreading center of the Red Sea to the collision zone of eastern Anatolia (Fig. 1). The history of the transform is not well established, but it is commonly accepted that the transform motion began 12 to 18 m.y.a. Matching the platformal sedimentary cover and some units of the basement complex across the transform, Quennell (1958) first recognised the left-lateral movement along the fault. He has estimated the total amount of displacement to be 107 km. From regional plate kinematics based on data from the Gulf of Aden and the Red Sea, Garfunkel and Ben-Avraham (1996) produced an independent estimation of the total motion of about 100 km. A regional kinematic model, which includes Eurasia, the African plate, the Somalian plate, and the Arabian shield, leads to a slip vector of about

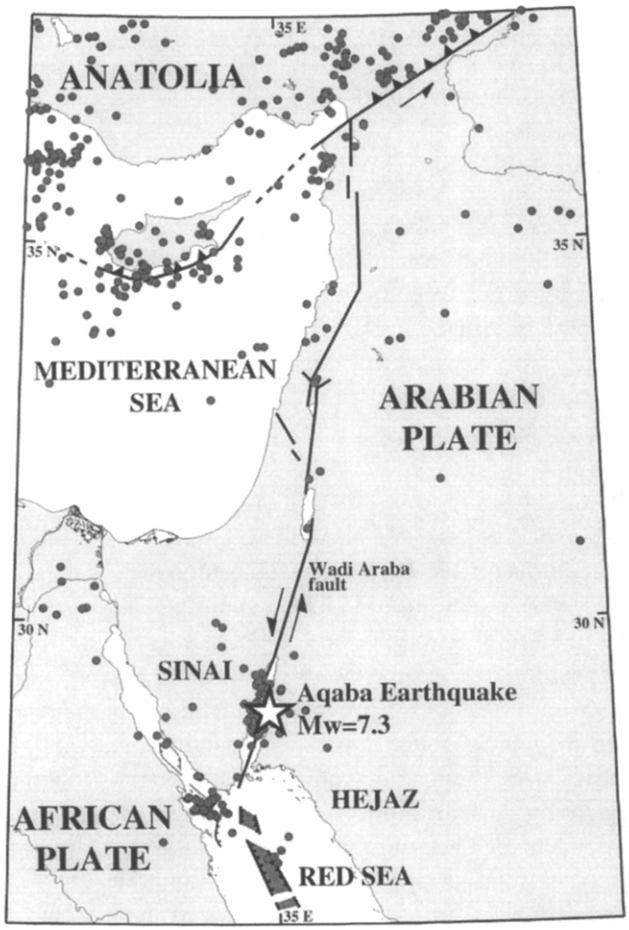

Figure 1. Present-day seismotectonic features in the Eastern Mediterranean area. Seismicity from 1960 to 1995 is reported from NEIC, including the 22 November 1995 earthquake and following aftershocks, for magnitudes greater than 3.

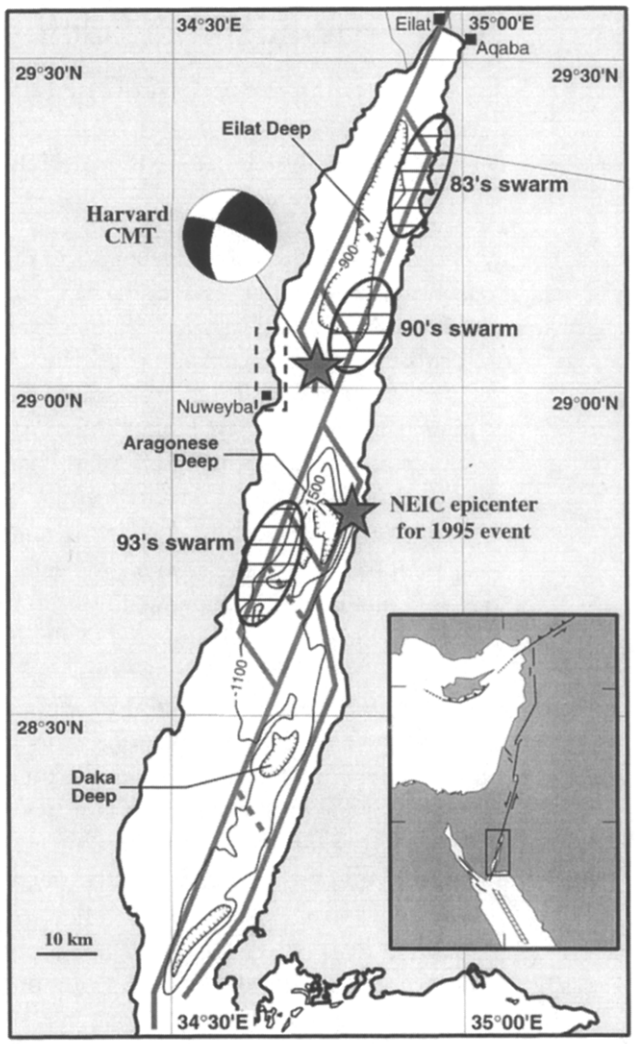

Figure 2. The locations of the swarms of 1983, 1990, and 1993 (Abou Karaki *et al.*, 1993; IPRG 1996), the location of the rupture initiation and the centroid of the 22 November 1995 earthquake. The tectonic features within the Gulf of Aqaba are adapted from Ben-Avraham (1985). The gulf is subdivided into three basins, from north to south: the Elat Deep (ED), the Aragonese Deep (AD), and the Daka Deep (DD). The dashed box north of Nuweyba indicates the area where ground failures have been observed.

8 to 10 mm/yr. for the southern part of the fault, south of the Dead Sea (Jestin *et al.*, 1994). Klinger *et al.* (1997) using a geomorphologic approach along the Jordan segment of the Wadi Araba fault estimated a velocity of 6 mm/yr for the last few tens of thousands years.

Along its entire length the Levantine fault is marked by several spectacular depressions corresponding to pull-apart basins, for example, the Dead Sea pull-apart. These basins are developing at jogs between successive segments of the fault. The Gulf of Aqaba is 180 km long but only 25 km wide, resulting from the succession of three pull-apart basins: the Dakar Deep, the Aragonese Deep and the Elat Deep, respectively, from the south to the north (Fig. 2). These basins are connected by *en echelon* strike-slip faults striking about N20 (Ben-Avraham, 1985). The component of normal motion on these faults that could accommodate a small amount of extension through the Gulf is still in debate (Ben-Avraham and Zoback, 1992). Although the Gulf is a very narrow structure, it is characterized by significant depths, reaching 1800 m deep in places, and is surrounded by the high mountain ranges of Sinai and Hedjaz, which are up to 2600 m in elevation. The total difference in height is over 4000 m, suggesting that tectonic processes are occurring faster than erosive processes to maintain this relief. Contrasting with the morphology of active tectonics within the gulf, background seismicity is scarce and characterized by swarms sequences (El-Isa *et al.*, 1984; Abou Karaki *et al.*, 1993; Shamir and Shapira, 1994). No large earthquake had occurred since the beginning of instrumental seismology and even during historical times very few earthquakes were reported for the region, even considering Sinai and Hedjaz (Ambraseys *et al.*, 1994).

The purpose of this article is to study the 22 November 1995 earthquake. A multidisciplinary approach allows us to gain a comprehensive view of the rupture process and its relation to the regional geodynamics. We looked at the previous background seismicity to better understand the location of the rupture initiation. Field investigation of the surface breakage along the Egyptian coast provided us with some clues about the morphological evolution of the gulf. A study of the aftershocks recorded by regional networks imposed some constraints on the geometry of the broken segments. Body waves recorded by the worldwide broadband seismic networks were inverted in order to compute the focal mechanism and the source time history of the main shock. Finally, combining the whole set of observations, we propose a coherent model of rupture for the 22 November 1995 earthquake in the Gulf of Aqaba that provides new insights into the regional geodynamics and active faulting in the Gulf of Aqaba.

Background Seismicity of the Gulf of Aqaba

The Gulf of Aqaba lies in an arid region; the Sinai peninsula and the Arabian shield are mostly a desert and, historically, only very few permanent human settlements have been located there. The seismologists who deal with historical seismicity are collecting macroseismic information from written documents found in the surrounding cities, which are in some cases rather far from the epicentral area. This can lead to mislocation when earthquakes are reported in places where they were felt and caused a lot of damage rather than in places where they have actually occurred. Data for the distribution of historical earthquakes are very sensitive to the population distribution. Therefore, for such desert regions it is difficult to establish an accurate catalogue of historical seismicity, and the completeness of such a catalogue will always be in debate. According to the reports concerning the M_W 7.3 earthquake that occurred in the Gulf of Aqaba in 1995, it appears that it was felt in all large cities in the area, for example, as far as Cairo or Jerusalem. Hence it seems reasonable that the catalogues are complete concerning the events with magnitude at least equal to 7 that have occurred in the Gulf of Aqaba during historical times, even if they were mislocated.

Nevertheless, modern studies (Abou Karaki, 1987; Ambraseys *et al.,* 1994) based on large and various sources of information agree that there is evidence for two or maybe three large earthquakes in the Gulf of Aqaba and the surrounding areas during the last 2000 years. The magnitudes of these events have been estimated at about 6.5 to 7, but they are poorly constrained because they are defined from the macroseismic data (Ambraseys *et al.,* 1994).

Since the beginning of the 80s the countries surrounding the Gulf of Aqaba have monitored local seismicity with regional networks. It appears that a low level of background seismicity is always present in the Gulf of Aqaba (Al Amri *et al.,* 1991). However, at least since the beginning of the instrumental period, the main characteristic of the seismicity in the Gulf of Aqaba is the occurrence of swarms. In fact three sequences of earthquakes that start and end gradually, without a single event dominating in size, have been observed (Fig. 2). Each time, the full process of increasing and decreasing seismic activity takes place within a few months. The first swarm occurred in 1983, and more than 1000 events were recorded in 3 months (Abou Karaki *et al.,* 1993; El-Isa *et al.,* 1984). The climax of this sequence was marked by three events with a magnitude (M_L) close to 5. Most of the events were located at the northeastern edge of the Elat Deep. In April 1990, a smaller swarm occurred in the central part of the gulf, in the area between the Elat Deep and the Aragonese Deep. During this sequence the magnitude reached 4.3 (M_L). A third earthquake sequence began in August 1993, following a moderate increase of the background seismicity over the month of July. This seismic activity produced peaks of magnitude of 6.1 (M_W), and more than 300 events with magnitudes of more than 3 occurred in the following weeks (Shamir and Shapira, 1994; Fattah *et al.,* 1997). This sequence was located in the southwestern part of the Aragonese Deep. Thus the location of the successive swarms moved from the north to the south of the Gulf of Aqaba (Fig. 2). It is noticeable that the last one, in 1993, was located close to the initiation of the event of 22 November 1995 on the western edge of the Aragonese Deep (Fig. 2).

Shamir and Shapira (1994) showed that the swarm activity defined distinct active segments around the different pull-apart basins forming the Gulf of Aqaba and induced shear stress onto segments that had not yet been broken.

It appears from this brief seismicity review of the Gulf of Aqaba that the regular level of seismicity is rather low but may increase significantly during brief swarm periods. Even if we extend the overview to the entire historical period, only two or three earthquakes with a moment release comparable to the 1995 event are known, but they are poorly documented.

Field Investigations

Surface ruptures related to the 22 November 1995 earthquake have been reported, both along the Egyptian coast of the gulf, close to the city of Nuweyba (Fig. 2) and along the Saudi Arabian coast. Field observations were conducted along the Saudi Arabian coast by Angelier *et al.* (1996). They observed a network of cracks affecting the quaternary formation along the coast, between 28°35′ N and 29°05′ N. The entire cracks system has a N20E trend and exhibits an *en échelons* arrangement, but mostly dip-slip displacement is reported all along the ground ruptures. Angelier *et al.* (1996) assumed that they observed primary coseismic rupture with a tectonic origin. Finally they propose that a trantensive regime with a direction of extension close to E–W takes place within the Gulf of Aqaba. We carried out a field survey during February 1996 along the Egyptian coast in

collaboration with the Egyptian Geological Survey and Mining Authority. Herein, we describe the ground ruptures that we observed along the Egyptian coast and discuss the tectonic origin of the ruptures.

The most striking ground rupture patterns were observed north of the city of Nuweyba, along the coastal road (Fig. 3). A system of cracks crosses the road with a N170E trend and continues for about 1 km toward the north. The fracture trend changes its orientation from N170E to N30E (Fig. 3). The system of cracks develops along the steep slopes of quaternary terraces. These terraces, which expose alternating sandy beach rocks sealed by coral reefs and alluvial fan conglomerates, are elevated by about 12 m above the sea (Fig. 3), demonstrating the vertical motions that take place within the gulf, in addition to the dominant strike-slip motion. Dominant top-to-the-east vertical offset is observed along these cracks, with a maximum offset of 20 cm (Fig. 3). The cracks present an *en échelon* arrangement along a N20E trend, with small overlappings between successive segments, which are connected by shorter N–S trending cracks forming extensional duplexes. However, we never found evidence of lateral offsets. On the other hand, we observed chattermark striations, which indicate systematic dip-slip displacements regardless of the strike of the crack (N–S to N30E).

Following the cracks system toward the north, the alluvial surface is entrenched by a wide talweg with a flat bottom (Fig. 4). The entrenchment is about 3 m high. As can be seen in Figure 4, the cracks system continues toward the north within the talweg groundfloor, in good accordance with the cracks previously described on the upper part of the alluvial surface. The vertical entrenchment shows that the cracks system is localized along a preexisting normal fault (Fig. 4). This normal fault affects the quaternary alluvial conglomerates forming the superficial deposits on the basement rocks composed of Cambrian sandstone and Cretaceous limestone. Close to the top of the escarpment, the fault splits into two branches, with a main fault plane dipping to the east and a conjugate compensation fault plane dipping to the west (Fig. 4). The main fault plane exposes chattermark striations made by pebbles, which indicate a dominant dip-slip displacement. The vertical offsets due to the 1995 earthquake do not exceed 10 cm on this part of the fault, but one can also observe an older cumulative vertical offset related to previous dip-slip displacement that is estimated to be about 1 m (Fig. 4).

No information is available yet about the timing of the oldest vertical offset, but since it affects basement rocks one could suggest that it is associated with a deep-seated fault. This observation is similar to the one made by Angelier *et al.* (1996) on the Arabian coast and could be interpreted in the same manner. However it is very unlikely that primary surface rupture affects both sides of the Gulf, so an alternative to the process of tectonic origin is needed to explain the cracks related to the 1995 earthquake as well as the previous one. As mentioned before, the trace of the rupture as

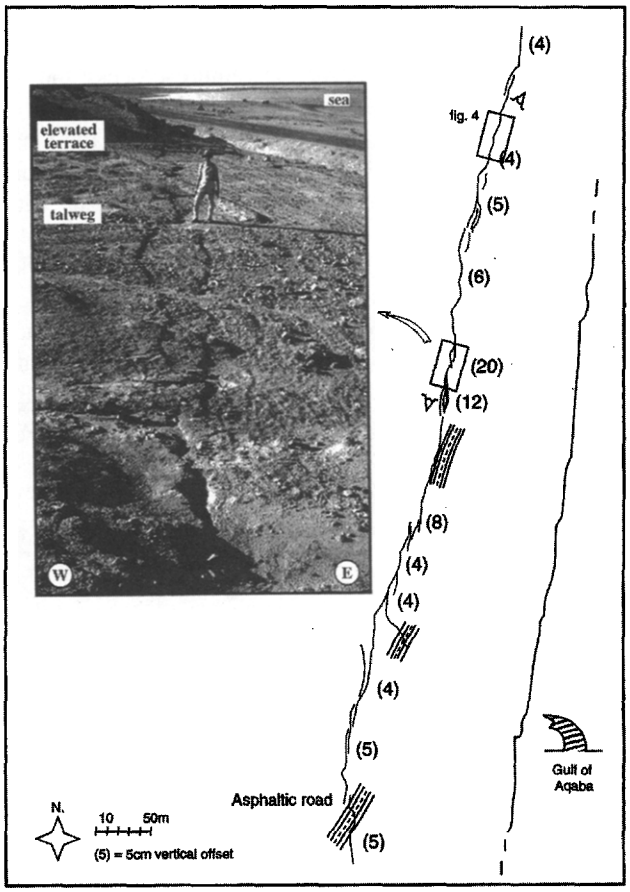

Figure 3. Map of the continuous ground ruptures observed along the Egyptian coast, north of Nuweyba. The vertical offset measured is reported in brackets. The second box indicates the location of the photo an example of ground rupture with the elevated terraces on the western side.

a whole follows a topographic high (the elevated terraces) to the west (photo in Fig. 3). During the main shock the elevated terraces collapsed to the east, opening cracks that were partly guided by a preexisting rupture in the basement. As no significant continuation of the trace of the rupture can be found after 1 km, neither toward the north nor toward the south along the beach, this supports the idea of the damping of the rupture. Therefore we propose that cracks we have observed north of Nuweyba are secondary features associated with subsiding of the coastal platform related to the 1995 event, rather than primary coseismic ruptures of broken segments.

In Nuweyba, gravity collapses guided by a preexisting basement fault were clearly documented for other ground ruptures reported by the Egyptian authorities (El-Hakim, 1996). In fact, behind the Oil Filling Station of Nuweyba, typical crescent-shaped open cracks provide evidence of a large landslide of quaternary fill. The cumulative vertical displacement of the quaternary deposits through the whole system of cracks is more than 2 m. According to people

living in the area, this terrifically noisy and dusty landslide occurred just after the main shock of 22 November 1995. We observed that the sliding of the terrace was guided by a preexisting surface corresponding to a large fault plane, visible because a quarry was excavated in this sector, denuding part of the fault plane. It can be followed for more than 200 m along the strike in the quarry in a roughly N–S direction.

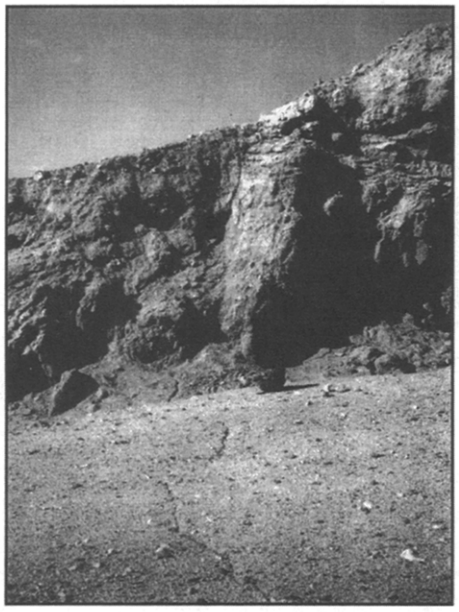

Figure 4. Photo and interpretative sketch of the cross section of the terrace (location in Fig. 3). The ground rupture continues from the upper part of the terrace into the groundfloor of the terrace. The cross section shows that the rupture took place on a preexisting fault surface. The vertical offset of about 10 cm due to the last event is visible, as is an older offset of about 1 m due to previous events.

It dips 60° to 70° to the east and it separates the granitic basement in the footwall from the quaternary terrace deposits in the hanging wall. Numerous slickenslides and chattermark striations affecting the footwall were observed along the fault plane, indicating direction and sense of movement.

We measured 26 striations in quaternary in-filling along the fault plane. Then we computed the stress tensor compatible with these striations (Célérier, 1995), selecting several groups of data corresponding to different stress tensor possibilities (Etchecopar *et al.*, 1981). We found a solution in good agreement with 20 striations (Fig. 5). This solution suggests an extensional stress field with a minimum horizontal stress (s3) striking roughly E–W and a stress ellipsoid shape ratio (R = s2 − s3/s1 − s3) close to zero, indicating radial extension (Fig. 5). In this case, since the most impor-

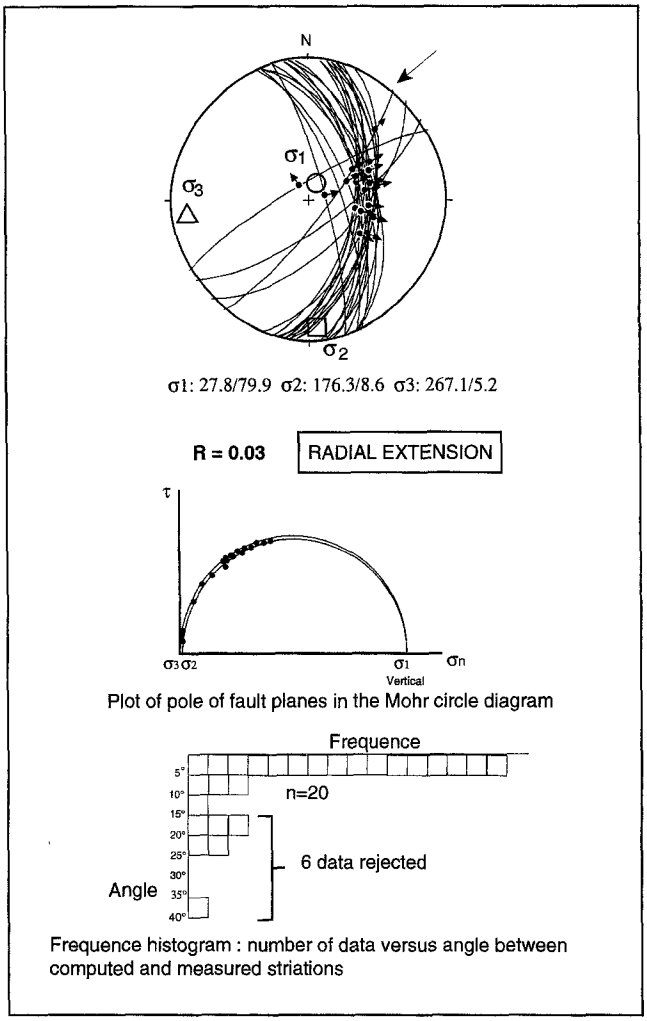

Figure 5. Stress tensor determination for 26 fault plane striations measured in the quarry of Nuweyba. The upper sketch shows observed striations with main stress axes computed. The arrow indicates the left-lateral striation (see text). The middle and lower sketches show, respectively, the Mohr diagram for the striations compatible with the stress tensor, and the histogram of angular differences between computed and observed slip directions.

tant driving force is the vertical stress, we assume that it can be associated with gravitational force. This result is consistent with landslide features we observed above the quarry. We should note that among the six data that do not fit with the computed stress tensor, five are not far from theoretical striations, and one exhibits a horizontal left-lateral component of slip (arrow in Fig. 5).

Finally, all field observations and stress calculation together confirm the assumption that large portions of quaternary terraces are subsiding along major fault scarps that bound the coast of the Gulf of Aqaba. This hypothesis is in good agreement with the observation of fossil fault scarps along the coast (Bowman and Gerson, 1986) and a marine shallow seismic profile performed within the gulf (Ben-Avraham, 1985). Gravitationally driven processes appear to dominate the coastal morphology of the Gulf of Aqaba.

Aftershocks Location

During the months following the main shock of 22 November 1995, thousands of aftershocks took place within the Gulf of Aqaba (IPRG, 1996; NRA, 1996). Because the coast of the Gulf of Aqaba is shared by four different countries, no single seismological network is able to monitor its high seismic activity as a whole. Nevertheless, each of the four countries surrounding the gulf (Egypt, Israel, Jordan, and Saudi Arabia) maintains its own network, and altogether 14 stations are installed temporally or permanently close to the epicentral area (maximum epicentral distance 150 km).

Thanks to the European–Mediterranean Seismological Center and the institutes of each country, we collected a data set of arrival times for about 1000 aftershocks that occurred during the months of November and December 1995. We checked that there was no accidental bias between timing of the different networks. In order to minimize location error, we used data only from stations with an epicentral distance of less than 150 km. Four stations from the Institute for Petroleum Research and Geophysics of Israel (IPRG) and 7 stations from the Natural Resource Authority (NRA) of Jordan fulfilled these conditions. Data from Saudi Arabia and Egyptian stations are available for only a few events. Even though some Jordanian stations are located far eastward of the gulf, the azimuthal aperture is rather low for most events, and the location of an earthquake is judged acceptable on the basis of the following criteria: (1) the rms must be less than 0.5 sec (we can not fix a lower rms criterion because no feedback is possible during the location process to check phase picking), (2) at least four *P*-phase readings and three *S*-phase readings are used in the hypocenter solution. The location is performed by using HYPO71 code (Lee and Lahr, 1975) with a tabular velocity model derived from models used by NRA and IPRG in this area. The HYPO71 output indicates that despite the critical conditions of location, 80% of the events finally retained are located with a horizontal error of less than 6 km. Figure 6 shows the final location for a set of about 350 aftershocks that fit the selected criteria.

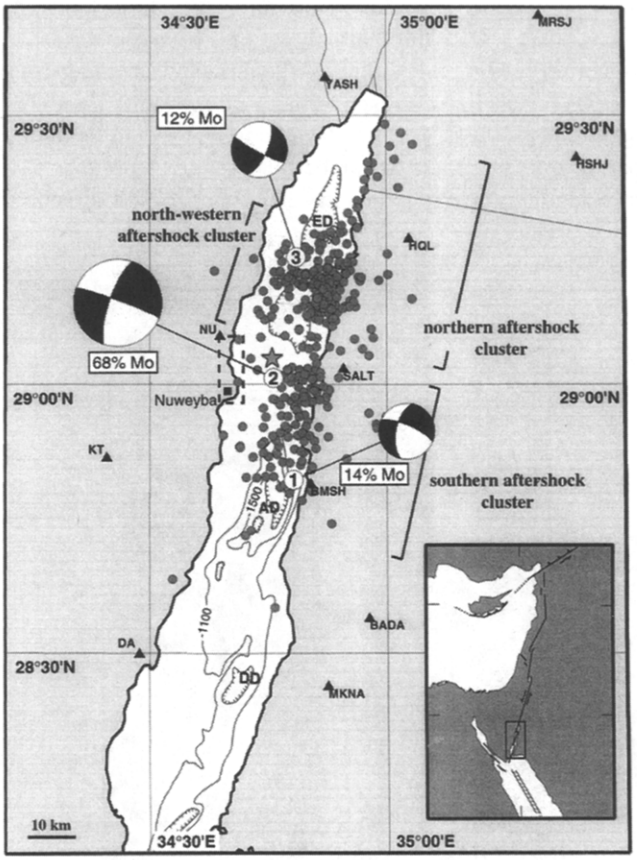

Figure 6. Aftershocks distribution for the 1995 Aqaba earthquake between 22 November and 31 December. The bulk of the aftershock distribution is located at the eastern edge of the gulf, excepted in the north where aftershocks extended westward. The focal mechanism for the three subevents and their location with respect to the aftershock clusters are also shown. The star close to the second subevent corresponds to the location of the centroid (Harvard CMT).

Although the total number of aftershocks we studied is smaller than the entire number of events recorded separately by each institute, the shocks' location is more reliable because of the merging of the data. We have an accurate picture of the aftershock distribution.

In Fig. 6 the epicenters are reported in a simplified chart of the bathymetry of the gulf. The first observation is that the length of the aftershock cloud, about 70 km, is comparable with the fault size we can expect for a magnitude 7.3 earthquake (Scholz, 1982). The general N–S orientation of the cloud also is in good agreement with the main structural trends all around the gulf (Eyal *et al.,* 1981; Ben-Avraham, 1985) and leads to an unambiguous choice for the further selection of the fault plane between the two possible nodal planes of focal spheres. The aftershocks distribution appears to form two clusters, one in the south and the other in the north.

In the south, events define a strip that is about 10 km wide and about 25 km long. It is well bounded on its eastern

and western edges. A few events are scattered out of the gulf and could be associated with reactivation of faults in reaction to the main shock or could correspond to an inaccurate location even if the above selection criteria were fulfilled. Nevertheless, this southern cluster of aftershocks is clearly located in the eastern part of the Gulf of Aqaba, along the Aragonese Deep main axis. North of this first cluster, lies the second cluster of aftershocks. It is separated from the first one by a zone with only a few events. The second cluster shows the largest concentration of events. Like the first one, it is characterized by a narrow strip pattern, with the same direction of elongation. Most of the events are located on the eastern edge of the Elat Deep, but we note that a significant number of the events is located on the western edge of the Elat Deep. These events show also a N–S elongated distribution that is used as *a priori* data during the body-wave inversion. They underly the fault escarpment that marks the western coast (Ben-Avraham and Zoback, 1992).

The larger amount of aftershocks in the northern cluster could be explained by the fact that we are on the extremity of the activated segments. Mendoza and Hartzell (1988) have shown that at the tips of the rupture the stress increases, and therefore a larger number of aftershocks occurs. Moreover, closer to the seismological stations the level of detection is better.

Due to the station distribution used in the location process, the depth for all these events could not be determined with good accuracy. Nevertheless the depths are distributed within the upper 20 km of the crust, and no particular pattern can be distinguished in this distribution.

Body-Wave Inversion

The CMT parameters of the 22 November 1995 event provided by Harvard (Dziewonski *et al.*, 1997) are as follows: strike 196°, dip 59°, and slip −15° (Fig. 2). The depth is 18 km. The scalar moment of 7.2×10^{19} N-m corresponds to M_W 7.3. The parameters of the centroid correspond to a sinistral strike-slip fault with a tiny normal component. This focal mechanism is in good agreement with the general tectonic setting of the gulf.

Data and Signal Processing

To determine the accurate geometry and history of the rupture we performed a simultaneous inversion of *P* waves and *SH* waves. We used 21 broadband teleseismic digital records from IRIS and GEOSCOPE networks, which allowed us to have reasonable azimuth coverage (Fig. 7) everywhere except in the southeastern quadrant where there is only one station available, MSEY. We compensate for this misdistribution of stations by applying different weight to each station, reinforcing the station of the southeastern quarter. We only use body waves from stations at an epicentral distance between 30° and 90° for *P* waves and 34° and 87° for *SH* waves to avoid strong, regionally variable, upper mantle and core phases arrivals, interfering with *P* and *SH* phases. The

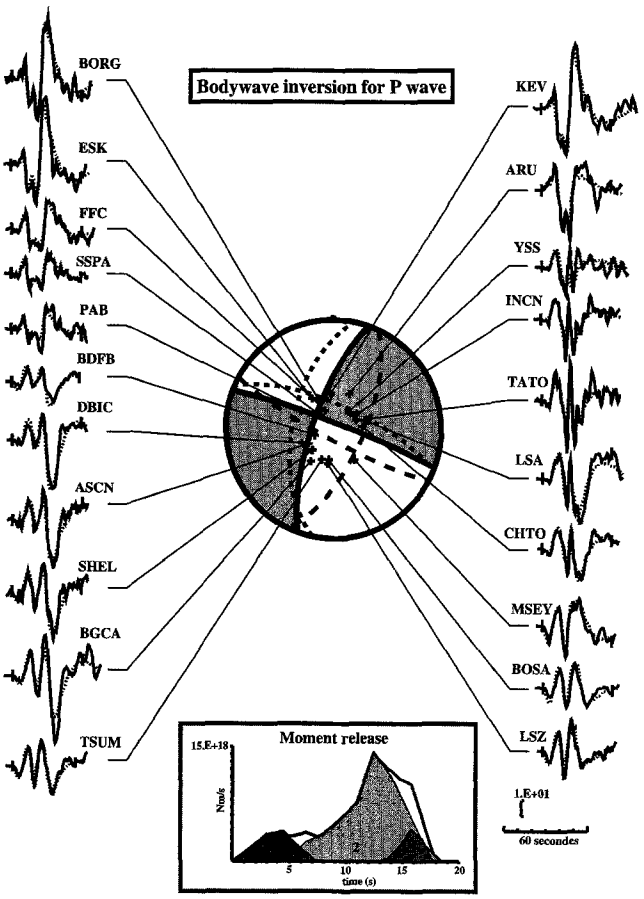

Figure 7. Final waveform modeling for the *P* waves from three sources. The focal mechanisms are represented for each subevent; the first one is a short dashed line, the second, a thick line, and the third, a long dashed line. The moment release is also reported for each subevent and for the total source (thick line).

inversion of focal parameters and far-field source time function is achieved by using the inversion process of Nabelek (1984). This process minimizes the square difference between the observed and calculated seismograms, following an iterative scheme.

Few details are known about the internal structure of the crust in the Gulf of Aqaba. Ben-Avraham (1985) proposed that in the southern part of the gulf a thinner crust was present and marked the transition between the spreading zone of the Red Sea and the shear zone of the Dead Sea fault. In this study, during the inversion process we modeled only direct waves and reflections at interfaces corresponding to velocity contrasts located above the source (Nabelek, 1984), such as the free surface, for example. Therefore we used a very simple one-dimensional velocity model that does not need to take into account the lower crust structure. We have fixed a water layer with a *P* velocity of 1.5 km/sec and no *S* waves, and a crust with a velocity of 6 km/sec and 3.46 km/sec for *P* and *S* waves, respectively. Similar approaches have been used previously in various tectonic contexts, for example, thrusting (Nabelek, 1985), subduction (Delouis *et*

al., 1997), or strike-slip faulting (Fuenzalida *et al.*, 1997). They show very good results for body-wave modeling.

In order to have a homogeneous data set we deconvolved each signal from its instrument response and filtered it with a bandpass filter between 1 sec and 100 sec for *P* waves and between 2 sec and 100 sec for *SH* waves. Then we resampled all data at two samples per second. During the inversion we used displacement records (integrated velocity signals) rather than velocity to reduce high frequencies generated by local structures. During the Nabelek process all records were normalized with a common gain to a distance of 40° from the epicenter.

The source parameters that we inverted for the process are the double-couple mechanism (strike, dip, slip), scalar moment, depth, source time function, and relative location, as well as time delay for each subevent if the complexity of the source required the introduction of subevents. The number of inverted parameters is large, causing concern about instability during the inversion process. *P*-wave and *SH*-wave radiation diagrams were rotated of 45°, with respect to each other, which helped significantly to constrain focal parameters when simultaneously using *P* and *SH* waves in the inversion.

Strategy of Inversion and Results

In the first step we determine the best point-source model at the epicenter. The duration of the moment liberation is 16 sec. The parameters of the point source are strike 196°, dip 75°, and slip −56°. The depth is 14 km, and the scalar moment M_o is 7.8×10^{19} N-m, corresponding to M_W 7.3. This solution shows a similar strike to the CMT solution but dips slightly more steeply and has a larger normal component. However, many problems of fit remain if we compare in detail observed and synthetic signals (Fig. 8). This is due to a higher complexity of the source, which cannot be reduced to one point-source but should involve several subevents.

To resolve the complexity of the rupture we looked first at directivity effects. We proceed by fixing the focal parameters as the best double-couple solution determined during the previous step, and we inverted 60 sec of the signal, for each station independently, in order to get the source time function at each station. This is equivalent to point source deconvolution (Kikuchi and Kanamori, 1982). As shown in Fig. 9, for some stations, shape and duration of the source time function are strongly azimuth dependent. In stations located to the north of the epicenter the source time function appears to be compact, with a duration about 15 sec. On the other hand, in stations located to the south of the epicenter the duration of energy liberation appears dilated, with a duration about 22 sec, with two distinct peaks of energy. The dependence on the azimuth is interpreted as a directivity effect of the rupture process. The source time history is contracted in the direction of propagation of the rupture, that is, the rupture propagated from the south to the north of the Gulf of Aqaba. The observation of two distinct peaks of energy at the southern stations is a clear indication of the existence of two or more significant subevents.

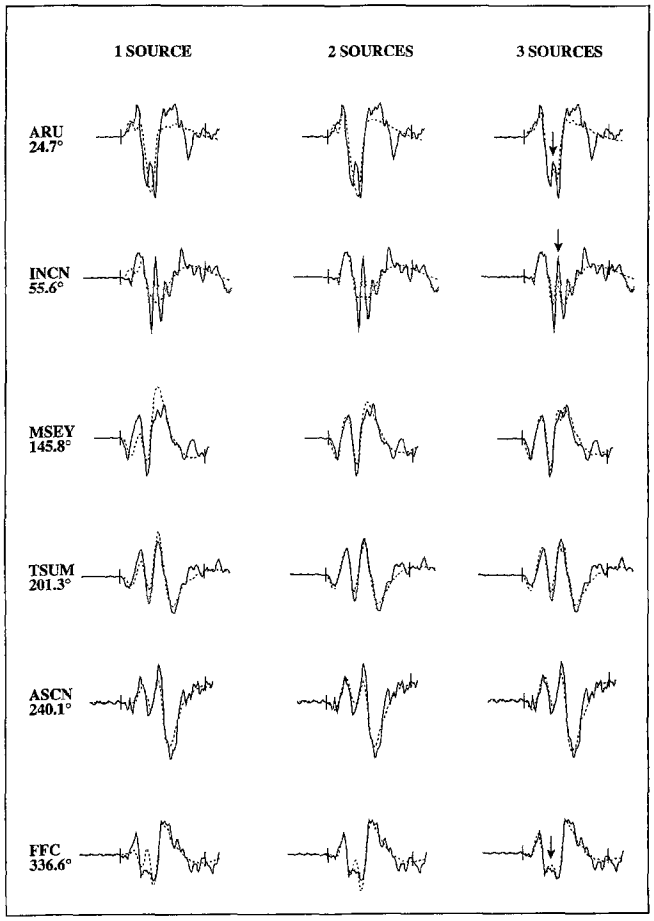

Figure 8. Comparison between observed (thick line) and synthetic (dashed line) seismograms for one, two, and three subevents at selected stations at various azimuths. The strong peak of energy in the center of the signal at ARU and INCN and the discrepancy in amplitude at FFC, indicated by the arrow, can be resolved only by modeling a third subevent.

In order to properly account for the directivity effect we inverted the source model for a propagating line source model, and we systematically tested the effects of different rupture velocities for a similar focal mechanism (Fig. 10). The negative sign of the rupture velocity indicates that the rupture is going in the direction opposite to the strike of the fault plane, confirming our previous observation of the directivity of the source. Moreover, a minimal value for the rms is obtained for a rupture velocity of 3 km/sec, which is in the range of the commonly accepted values. Hence we used this value of rupture velocity in the rest of the inversion process.

Next we performed an inversion with two propagating line sources, as was suggested by the azimuthal variation of the source time function (Fig. 9). The initiation of the rupture is fixed at 28.83° N and 34.79° E, the epicentral location provided by the PDE monthly listing of the NEIC, which was computed using data from networks all around the world.

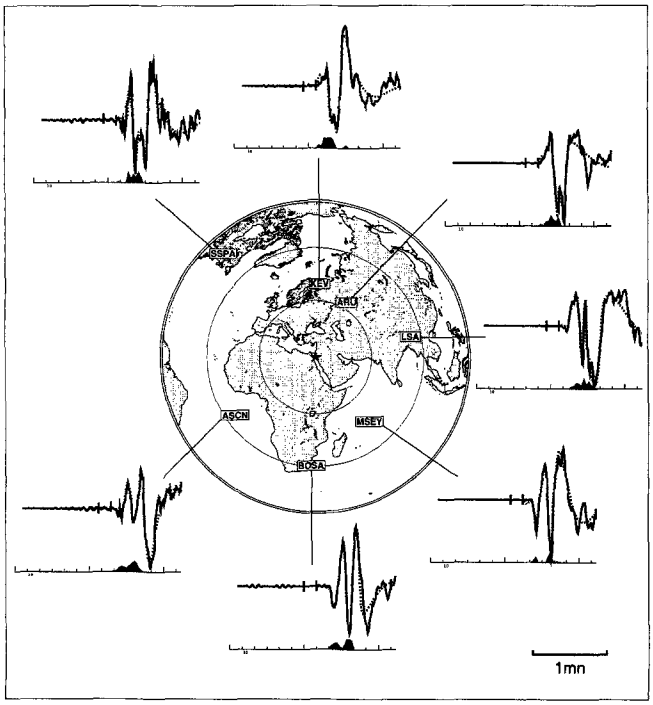

Figure 9. Representative variation of the shape and duration of the source time function with respect to the source-station direction. Each signal (60 sec) is inverted singularly for the same fixed focal parameters in order to determine directivity effects and number of subevents.

Other locations from different regional networks are found scattered close to this location (El-Hakim, 1996; IPRG, 1996; NRA, 1996; Fattah *et al.*, 1997). The NEIC epicenter was deemed sufficient since the inversion process is not very sensitive to small mislocation because it uses mainly the relative time lag between the different inverted signals. The relative position of each subevent is determined from the inversion process with respect to the initial position, leading to the whole geometry of the rupture. Initially, to reduce the number of parameters to be inverted, we constrain *a priori* the focal mechanism of the first event to be in agreement with the first motion of the teleseismic *P* waves. In this way the inversion of the parameters for the second subevent is more constrained because we decrease the trade-off between the different parameters.

The position of the second subevent with respect to the first one is not easy to establish because a variation of a few kilometers of the position have only small consequences on the shape and amplitude of the signal. Figure 11 shows the rms variations between observed and synthetic seismograms for a regular grid of positions (distance and azimuth) of the second subevent with respect to the first one. It is clear that the rms is minimal when the second subevent is to the northwest of the first subevent. Moreover, this geometry is reinforced by the location of the aftershocks; the southern cluster covers all the Aragonese Deep and not only its western edge, implying the activation of both sides of the deep (Fig. 6).

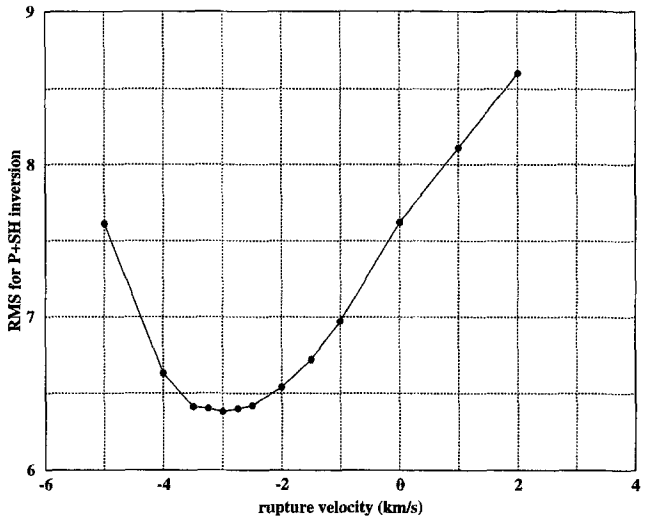

Figure 10. Variation of the rms during simultaneous inversion of *P* and *SH* waves with the same focal mechanism but different rupture velocity. Negative rupture velocity corresponds to rupture northward.

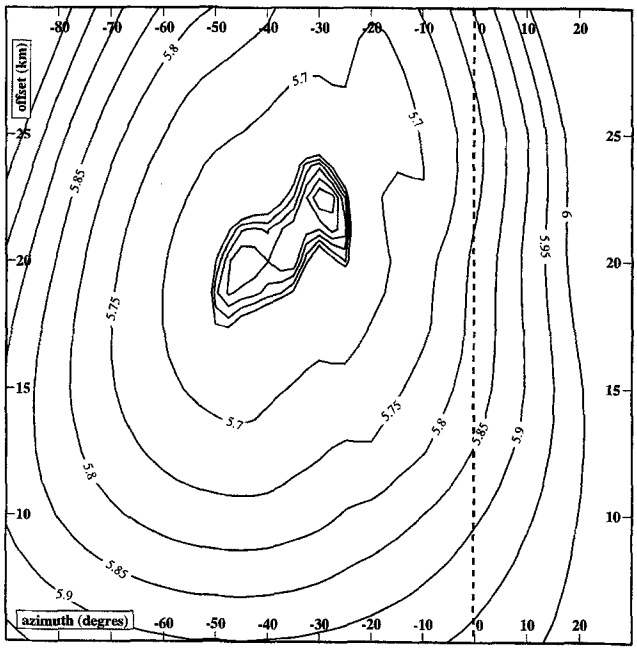

Figure 11. Variation of the rms during the simultaneous inversion of *P* and *SH* waves for different position of the second subevent with respect to the first one (located at 0,0). The dashed line indicates the azimuth 0° N. Minimal values are obtained for a second subevent located between 15 and 27 km in azimuth between N15°W and N50°W.

Moreover, the location of the centroid from PDE shows that in fact the centroid is located northwest of the initiation of the rupture.

The introduction of the second subevent improved our solution, as shown in Fig. 8. Nevertheless, it appears that for

stations located north of the earthquake (FFC, ARU, and INCN, for example), there is a strong misfit between observed and synthetic seismograms. For stations located east of the earthquake (ARU and INCN in Fig. 8) we observe a peak of energy in the middle of the signal that is not modeled. Similarly, for the station located to the west of the earthquake (FFC in Fig. 8) we see that the amplitude of the synthetic signal does not correspond to the observed signal. Because this misfit is coherent among several stations it demonstrates that we are not trying to fit noise or signal derived from local structures. Hence these data suggest that a third subevent has to be introduced to take into account the discrepancy between the observed and computed signals. Here again, using the location of the aftershocks, and mostly the westward extension of the northern cluster, we fixed *a priori* some parameters, namely, the relative location of the third subevent. This way we decreased the possibility of a trade-off between the other parameters during the inversion process. The focal mechanism determined for this third subevent is sinistral strike-slip with a very small normal component.

At each step of the inversion we took care of the *a priori* information we used to limit the trade-off between inverted parameters. In fact, we considered a solution valid only if it was stable when afterward we liberated the *a priori* parameter. Otherwise, we rejected the solution and started again, changing the *a priori* parameter.

Finally, we model the 22 November 1995 earthquake by subdividing the main shock into three subevents (Table 1). In that way we were able to explain most of the signal recorded on the broadband stations of the worldwide network (Figs. 7, 8, and 12). The time delay between the first and the second subevent is 5.0 sec, and between the first and third subevent is 11.7 sec. The total duration of the source time function is 18.7 sec. These results are in good agreement with results proposed by Wdowinski and Ben-Avraham (1997) for the time delay between the two first subevents and the global duration of the source function. The relative location of the three subevents is also determined during the inversion. Hence, as mentioned before, mainly for the last event, the location is not definite. Nevertheless, we performed tests with three aligned sources that showed that for the same source parameters, the solution we proposed better fits the details of the signal. In fact, with respect to the source parameters, there are few possible solutions because the external constraints are strong. Pinar and Türkelli (1997) have proposed that the first shock was dip-slip, but this seems to contradict the focal mechanism (Fattah *et al.*, 1997) derived from first motion, including local data.

Discussion

Review of the background seismicity reveals that the usual level of seismicity is low within the Gulf of Aqaba. During the historical period only two or three large events were documented. Since the instrumental monitoring began, seismic activity has been low and was disrupted only by the three seismic swarms of 1983, 1990, and 1993. Each seismic episode appears to have been concentrated on a specific segment of the fault system. During the period preceding the 1995 earthquake the swarms migrated southward and were located at the end, the middle, and the beginning of the 1995 rupture. The energy released by the largest swarm, in 1993, is only some hundredth of the energy of the 1995 earthquake, but this swarm sequence seems to have been a preparation for the 1995 rupture by concentrating stress on the 1995 broken segments (Figs. 2 and 6).

This earthquake is the largest instrumentally documented event that has occurred in the Gulf of Aqaba. From the body-wave inversion and the aftershock distribution we propose the following rupture model (Figs. 6 and 13). The total moment liberation is 7.42×10^{19} N-m, distributed in three subevents. The rupture initiated on the fault bordering the eastern edge of the Aragonese Deep. This first subevent is M_W 6.7, corresponding to 14% of the total energy released during the earthquake. Its focal mechanism is mainly sinistral strike-slip with a small amount of normal motion in agreement with its location on the eastern border of the Aragonese basin. We could propose that the rupture started on the eastern edge of the deep because the western edge had already been broken during the swarm activity of 1993. The main shock started 5.0 sec later on the opposite edge of the Aragonese basin, breaking the segment that connects the Aragonese Deep to the Elat Deep in the north. Similar jumps have already been observed on other strike-slip faults. For example, jumps of a few kilometers were documented in the 1992 Landers earthquake (Zachariasen and Sieh, 1995). The second subevent was M_W 7.2, corresponding to 68% of the total energy released. The focal mechanism is nearly pure sinistral strike-slip faulting. Here again, we propose that the

Table 1
Source Parameters

Event No.	Strike (degrees)	Dip (degrees)	Rake (degrees)	Depth (km)	M_0 (dyne-cm) $\times 10^{26}$	Δt* (sec)	Dist† (km)	Azim‡ (degrees)
1	191.6	58.6	−21.2	18.80	1.07	0.0	0.0	0.0
2	199.3	74.3	−5.0	18.65	5.40	4.97	22.3	−27.7
3	24.7	67.2	−8.5	5.15	0.953	11.78	40.5	1.8

*Δt, time delay with respect to the initiation of the rupture.
†Dist, horizontal distance of the event to the nucleation point.
‡Azim, azimuth of the line joining the nucleation point to the subevent, with respect to the north.

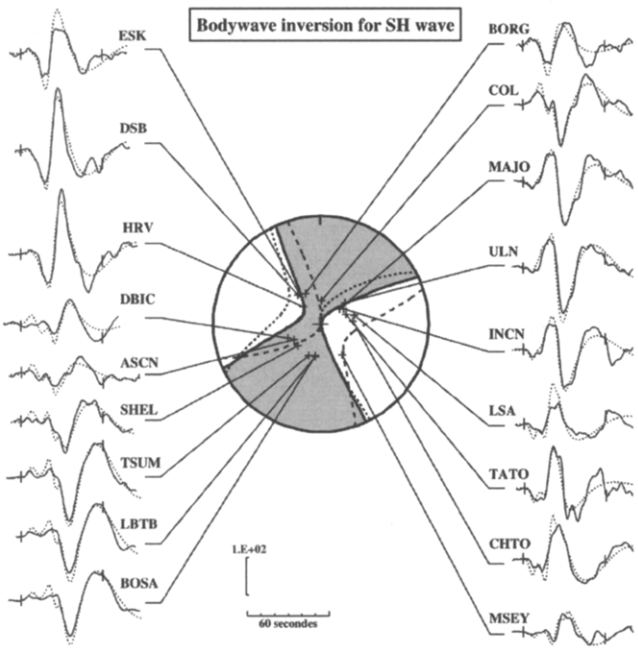

Figure 12. *SH*-wave modeling corresponding to the final source model.

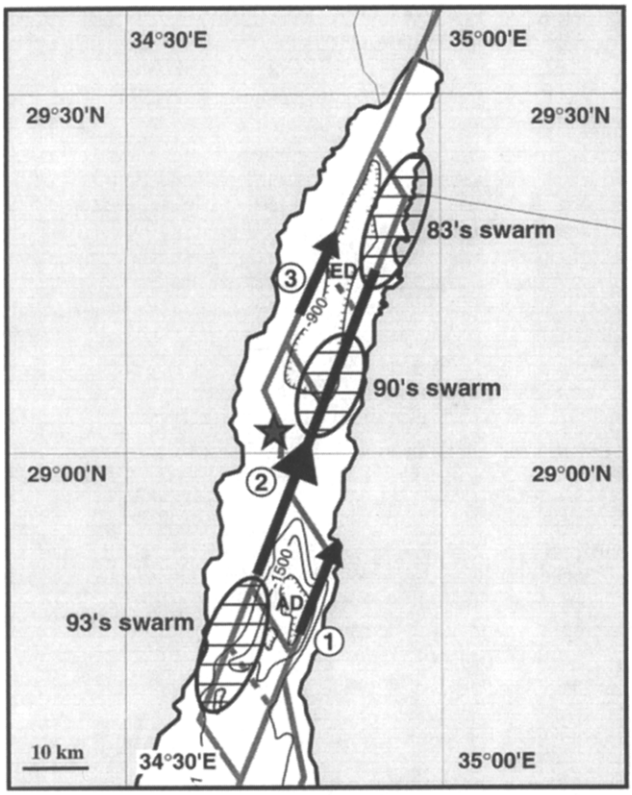

Figure 13. Model of the rupture (black lines) of the 22 November 1995 earthquake in the Gulf of Aqaba. Gray lines shows fault segments identified from bathymetric charts (adapted from Ben-Avraham, 1985), and striped ellipses correspond to swarm location. The star indicates the location of the centroid (Harvard CMT).

geometry of the rupture is controlled by the previous seismic activity within the gulf; the main shock initiated at the northern extremity of the area where the swarm of 1993 took place and stopped at the beginning of the area where the swarm of 1983 took place. The main rupture seems to go through the area related to the swarm of 1990, and the lower number of aftershocks in this zone could be related to the fact that the stress had already been partially released. Finally, a third subevent occurred 11.8 sec after the beginning of the rupture. This subevent was M_W 6.7, corresponding to 12% of the total energy released. The location of this last subevent is difficult to establish with accuracy due to its signal weakness, but the results of the body-wave inversion are in favor of location on the western edge of the Elat Deep. In fact, from the inversion we get a fault plane dipping 67.2° toward the East. This dipping is in good agreement with seismic profile in the Gulf of Aqaba (Ben-Avraham, 1985). Moreover, the distribution of the aftershocks extends clearly westward in the Elat Deep and seems to be associated with the activation of the western segment. Finally, the swarm of 1983 must have released a large part of the stresses at the northern end of the central segment, leading to the jump of the rupture to the western segment where most of the stress accumulated.

The proposed model for the 1995 earthquake, summarized in the Figure 13, shows dominant strike-slip motion with respect to normal motion. Surface ruptures that are located in the sediments of the coastal platform formed by alluvial fans and coral reef correspond to dip-slip. This is mainly interpreted as the result of gravity subsidence in response to the earthquake shaking. Moreover, the lack of aftershocks where the surface ruptures have been observed reinforces this interpretation. It does not mean that no extension at all occurred in the Gulf of Aqaba but rather that strike-slip is the dominant tectonic process on all main fault segments in the gulf, leading to the formation of three pull-apart basins. The normal motion is accommodated by smaller events, such as the 1993 event (M_W 6.1) characterized by an almost pure normal focal mechanism (Dziewonski *et al.*, 1994), or the tiny normal component of the focal mechanism of the 1995 earthquake.

The 22 November 1995 earthquake demonstrates the fact that large and destructive earthquakes can occur in the Gulf of Aqaba. It appears that in 15 years, through the swarm activity and this last big earthquake, most of the active segments within the gulf have been involved in the seismic activity. Similar tectonics continues toward the north, and we believe that similar earthquakes could occur there also. If we consider scaling laws for earthquakes (e.g., see Wells and Coppersmith, 1994), it appears that the displacement due to small events, however numerous, will never be able to account for a large event. Since there are at most four events, including the 1995 event, having a magnitude greater than 6.5 for the past 2000 years, we can assume an upper limit for the cumulative displacement of about 8 m (Scholz, 1982). This means a maximum velocity of about 4 mm/yr. The velocity derived from plate tectonics models is about

8 to 10 mm/yr (e.g., see Jestin *et al.*, 1994). This emphasises that the level of seismicity is at most normal, if not low, compared with what could be expected from the plate tectonics models. Moreover, field investigation on the Egyptian coast have revealed the weakness of the coastal platform and the risk of large collapses if it is submitted to the strong shaking associated with earthquakes. All of these parameters have to be considered for any serious study of the seismic risk evaluation of the Gulf of Aqaba.

Acknowledgments

We are very indebted to all the staffs of the Natural Resource Authority of Jordan, the Geophysical Institute of Israel, of the Egyptian Geological Survey, and Mining Authority and of the King Saud University of Saudi Arabia for their essential work in the daily monitoring of seismic activity. To all of them and also to the staff of the Euro-Mediterranean Seismological Center, which collects and distributes the data, a very grateful thanks. We thank also the Egyptian Geological Survey and Mining Authority, which provided all facilities during the field work. Drawings were made mostly using GMT free software. Constructive comments made by L. Dorbath and two anonymous reviewers markedly improved the manuscript.

References

Abou Karaki, N. (1987). Synthèse et carte sismotectonique des pays de la bordure orientale de la Méditerranée: sismicité du système de failles du Jourdain-Mer Morte, *Ph.D. Thesis,* University of Strasbourg, France.

Abou Karaki, N., L. Dorbath, and H. Haessler (1993). La crise sismique du golf d'Aqaba de 1983: implication tectonique, *C. R. Acad. Sci. Paris* **317,** 1411–1416.

Al Amri, A. M., F. R. Schult, C. G. Bufe (1991). Seismicity and aeromagnetic features of the Gulf of Aqaba (Elat) region, *J. Geophy. Res.* **96,** 20179–20185.

Ambraseys, N. N., C. P. Melville, R. D. Adams (1994). *The Seismicity of Egypt, Arabia and the Red Sea, a Historical Review,* Cambridge U Press.

Angelier, J., P. Hancock, M. Al-Dail, N. Sha'at (1996). Etude seismotectonique de failles actives entre Haql et Maqnah, Arabie Saoudite: Trace du séisme du Golfe d'Aqaba (22 Nov. 1995) (Abstract), in *RST 16th* 10–12 April, Orléans, France.

Ben-Avraham, Z. (1985). Structural framework of the gulf of Elat (Aqaba), northern Read Sea, *J. Geophys. Res.* **90,** 703–726.

Ben-Avraham, Z., and M. D. Zoback (1992). Transform-normal extension and asymmetric basins: an alternative to pull-apart models, *Geology* **20,** 423–426.

Bowman, D., and R. Gerson (1986). Morphology of the latest quaternary surface faulting in the gulf of Elat region, Eastern Sinai, *Tectonophysics* **128,** 97–119.

Célérier B. (1995). Tectonic regime and slip orientation of reactivated faults, *Geophys. J. Int.* **121,** 143–161.

Delouis, B., T. Monfret, L. Dorbath, M. Pardo, L. Rivera, D. Comte, H. Haessler, J. P. Caminade, L. Ponce, E. Kausel, and A. Cisternas (1997). The M_W = 8.0 Antofagasta (Northern Chile) earthquake of July 30, 1995: a precursor to the end of the large 1877 gap, *Bull. Seis. Soc. Am.* **87,** 39–66.

Dziewonski, A. M., G. Ekstrom, and M. P. Salganik (1994). Centroid-moment tensor solution for July–September 1993, *Phys. Earth Planet. Inter.* **83,** 165–174.

Dziewonski, A. M., G. Ekstrom, and M. P. Salganik (1997). Centroid-moment tensor solution for October–December 1995, *Phys. Earth Planet. Inter.* **101,** 1–12.

El-Hakim, B. A. (1996). The Aqaba 95 Earthquake—a Quick Review, report of the Egyptian Geological Survey and Mining Authority.

El-Isa Z. H., H. M. Merghelani, and M. A. Bazzari (1984). The Gulf of Aqaba earthquake swarm of 1983 January–April, *Geophys. J. R. Astr. Soc.* **78,** 711–722.

Etchecopar, A., Vasseur, G., Daigniers, M. (1981). An inverse problem in microtectonics for the determination of stress tensor from fault striation analysis, *J. Struct. Geol.* **3,** 51–65.

Eyal, M., Y. Eyal, Y. Bartov, and G. Steinitz (1981). The tectonic development of the western margin of the gulf of Elat (Aqaba) rift, *Tectonophysics* **80,** 39–66.

Fattah, A. K. A., H. M. Hussein, E. M. Ibrahim, and A. S. Abu el Atta (1997). Fault plane solutions of the 1993 and 1995 Gulf of Aqaba earthquakes and their tectonic implications, *Annali di Geofisica* **40,** 1555–1564.

Fuenzalida H., L. Dorbath, A. Cisternas, H. Eyidogan, A. Barka, L. Rivera, H. Haessler, H. Philip, and N. Lyberis (1997). Mechanism of the 1992 Erzincan earthquake and its aftershocks, tectonics of the Erzincan Basin and decoupling on the North Anatolian Fault, *Geophys. J. Int.* **129,** 1–28.

Garfunkel, Z., and Z. Ben-Avraham (1996). The structure of the Dead Sea basin, *Tectonophysics* **266,** 155–176.

IPRG (Institute for Petroleum Research and Geophysics of Israel) (1996). Seismological bulletin 1996: earthquakes in and around Israel.

Jestin, F., P. Huchon, and J. M. Gaulier (1994). The Somalia plate and the East African Rift System: present-day kinematics, *Geophys. J. Int.* **116,** 637–654.

Kikuchi, M., and H. Kanamori (1982). Inversion of complex body waves. *Bull. Seis. Soc. Am.* **72,** 491–506.

Klinger, Y., J. P. Avouac, and N. Abou Karaki (1997). Seismotectonics of Wadi Araba fault (Jordan) (Abstract), in *EGS 22th General Assembly* 21–25 April, Vienna, Austria, Annales Geophysica Sup., 15.

Lee, W. H. K., and J. C. Lahr (1975). HYPO71, a computer program for determining hypocenter, in *U.S. Geol. Surv. Open-File Rept.,* 75-311.

Mendoza, C., and S. H. Hartzell (1988). Aftershock patterns and main shock faulting, *Bull. Seis. Soc. Am.* **78,** 1438–1449.

Nabelek, J. (1984). Determination of earthquake source parameters from inversion of body waves, *Ph. D. Thesis,* Massachusetts Institute of Technology, Cambridge, Massachusetts.

Nabelek, J. (1985). Geometry and mechanism of faulting of the 1980 El Asnam, Algeria, earthquake from inversion of teleseismic body waves and comparison with observations, *J. Geophy. Res.* **90,** 12713–12728.

NRA (National Resource Authority of Jordan) (1996). Seismological bulletin 1996: earthquakes in Jordan and adjacent areas.

Pinar, A., and N. Türkelli (1997). Source inversion of the 1993 and 1995 Gulf of Aqaba earthquake, *Tectonophysics* **283,** 279–288.

Quennell, A. (1958). The structural and geomorphic evolution of the Dead Sea rift, *Quaterly J. Geol. Soc. London* **114,** 1–24.

Scholz, C. H. (1982). Scaling laws for large earthquakes: consequences for physical models, *Bull. Seis. Soc. Am.* **72,** 1–14.

Shamir, G., and A. Shapira (1994). Earthquake sequences in the gulf of Elat (Abstract), in *IASPEI 27th General Assembly,* Wellington, New Zealand.

Wells, D. L., and K. J. Coppersmith (1994). New empirical relationships among magnitude, rupture length, rupture width, rupture area and surface displacement, *Bull. Soc. Seis. Am.* **84,** 974–1002.

Wdowinski, S., and Z. Ben-Avraham (1997). Tectonics constraints on the nucleation, rupture, and arrest of the 1995 Gulf of Elat (Aqaba) Earthquake (Abstract), in *IASPEI 28th General Assembly,* Thessaloniki, Greece.

Zachariasen, J., and K. Sieh (1995). The transfer of slip between two en echelon strike-slip faults: a case study from the 1992 Landers earthquake, southern California, *J. Geophy. Res.* **100,** 15281–15301.

EOST, UMR CNRS-ULP 7516
5, Rue René Descartes
F-67084 Strasbourg, France

Manuscript received 5 January 1998.